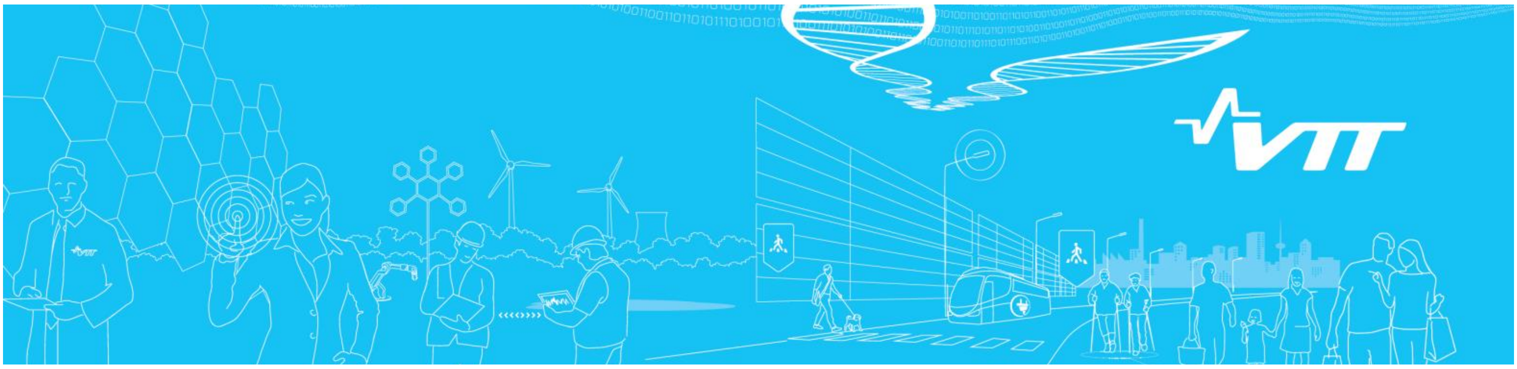

RESEARCH REPORT

VTT-R-04076-15

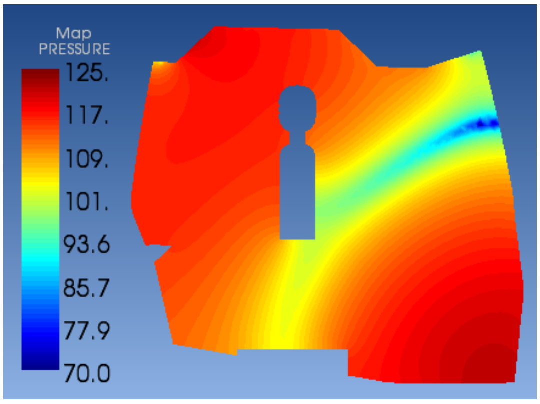

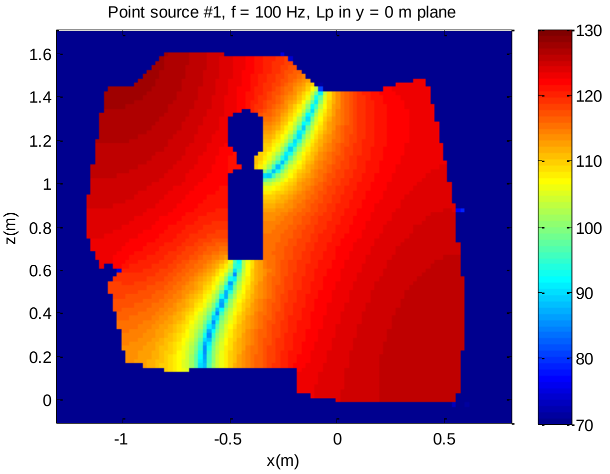

SIMPRO VTT Subproject Task 2.5 Deliverable

Acoustic simulation in HPC and cloud environment

Authors: Seppo Uosukainen, Denis Siponen

Confidentiality: Public

Report's title	
Acoustic simulation in HPC and cloud environment	
Customer, contact person, address Tekes, Matti Säynätjoki Kyllikinportti 2, P.O. Box 69, FI-00101 Helsinki, FINLAND	**Order reference** Tekes: 40204/12
Project name Computational methods in mechanical engineering product development	**Project number/Short name** 100553 (78634) / SIMPRO
Author(s) Seppo Uosukainen, Denis Siponen	**Pages** 26
Keywords boundary element method, interior problem	**Report identification code** VTT-R-04076-15

Summary

Acoustic simulation test case was performed with Kuava Oy's software application Waveller Cloud. It uses CompA algorithm which is based on the boundary element method (BEM) for solving the acoustic wave equation in frequency domain. BEM is mostly used and best applicable to exterior problems and in this context it was used to interior problems where it is not as efficient as the finite element method (FEM). Furthermore, a true fluid-structure interaction and propagating waves in structures cannot be modelled only using BEM as they can with coupled vibro-acoustic FEM, only locally reacting boundary conditions (impedance) for acoustic fields can be associated to the boundary structures. This may cause errors with individual strongly coupled near-by surface parts especially if the individual surface properties deviate much from each other.

The case study, Valtra cabin T888M, was concentrated on the sound field distributions produced by an acoustic point source into the interior of a tractor cabin, and simulation of material utilization in three inner roof elements for which calculated results exist based on FEM simulations in NOVI project. Probably the main reason for the largely different results of the sound pressure level distributions in the cabin at 100 Hz of Waveller Cloud calculations, compared to those of Actran, for the inner roof case 1 is treating separately and as locally reacting the centre and outer parts of the inner roof. Also the small deviations in the sound field distributions for the inner roof cases 2 and 3 are probably due to the handling of some affecting things in a different manner in FEM and BEM models. Otherwise, these computed results are tolerably in agreement. Using BEM in interior problems is very sensitive to proper impedance definitions of the boundaries.

Confidentiality	Public

Espoo 7.9.2015

Written by	**Reviewed by**	**Accepted by**
Seppo Uosukainen, Principal Scientist	Jukka Tanttari, Principal Scientist	Johannes Hyrynen, Head of Research Area

VTT's contact address

VTT Technical Research Centre of Finland Ltd, P.O. Box 1000, FI-02044 VTT, FINLAND

Distribution (customer and VTT)

Tekes/Matti Säynätjoki, 1 copy
VTT/archive, 1 copy

Preface

This report is one deliverable of VTT Subproject of SIMPRO project (Computational methods in mechanical engineering product development), funded by TEKES, industry, VTT and collaborating universities. The project runs from 2012 to 2015.The main objective of the project is to lower the step to utilise computational methods – including single complex simulations and analysis, and large series of computations – in large-scale computations using efficient and convenient computational systems, tools, and practices. The main objective of Task 2 (Optimization, design studies and analyses) of the project is to help the engineer to utilise available computational resources to be used for computation processes which will require several runs of an individual case. This deliverable is the outcome of Task 2.5 (Acoustic simulation in HPC and cloud environment).

Espoo 7.9.2015

Authors

Contents

1. Introduction

Running computational optimisation during design process and for practical models can be very computationally resource intensive. An optimisation process case may require hundreds, thousands, or tens of thousands of simulation runs, each producing large amount of numerical data. In addition, the large number of simulation runs can take long time to run if massive parallelisation cannot be utilised. Especially acoustic simulation and optimisation at high audio frequencies needs excessive computing power.

2. Goal

In this subtask the goal is to perform an acoustic simulation test case with Kuava Oy's new software application Waveller Cloud (under development), based on the boundary element method, to give valuable information of the possibilities to extend the acoustic simulations in the whole audio frequency range. The software is available for local as well as cloud computing. One goal is to evaluate the applicability of this software to the acoustic simulation in these environments.

It must be noted that not all goals could be met in this subtask. Cloud environment could not be used in this subtask and instead, a desktop computed was used in calculation. Also the frequency range was limited to 80 – 400 Hz.

3. Description

The study contains a pre-study and one test case. The case study is concentrated on the noise emission from an acoustic point source into the interior of a tractor cabin, and simulation of material utilization in the inner roof element.

4. Pre-study considering used computation methods

The mathematical background of CompA algorithm, used in the Kuava Oy's software Waveller Cloud [1], is presented. This presentation is based on Kuava Oy's documents [2, 3] and personal communication [4]. Before that, some basic theory behind the software is presented. This contains the Helmholtz–Huygens integral, strong and weak problem formulations, the Galerkin method, and how the boundary element method, used in Kuava Oy's software, is bound to these concepts.

4.1 Helmholtz–Huygens integral

The linearized non-homogeneous wave equation for sound pressure p in a homogeneous, ideal (i.e., lossless) fluid without static flow is

$$\nabla^2 p(\vec{r},t) - \frac{1}{c_0^2}\frac{\partial^2 p(\vec{r},t)}{\partial t^2} = -\rho_0 \frac{\partial q'(\vec{r},t)}{\partial t} + \nabla \cdot \vec{f}(\vec{r},t), \tag{1}$$

where $\vec{r}$ is spatial coordinate vector, t is time, and c_0 and ρ_0 are the linearized speed of sound and the static density of the fluid. Terms q' and $\vec{f}$ denote the monopole source distribution and dipole source distribution per unit volume in the fluid. Also other source types can be defined [5].

Let us consider a fluid volume *V* with a smooth closed boundary surface *A* and a unit normal vector $\vec{e}_n$ at the boundary surface pointing towards volume *V* as presented in Figure 1. *V* can be outside *A* (exterior problem) or inside *A* (interior problem).

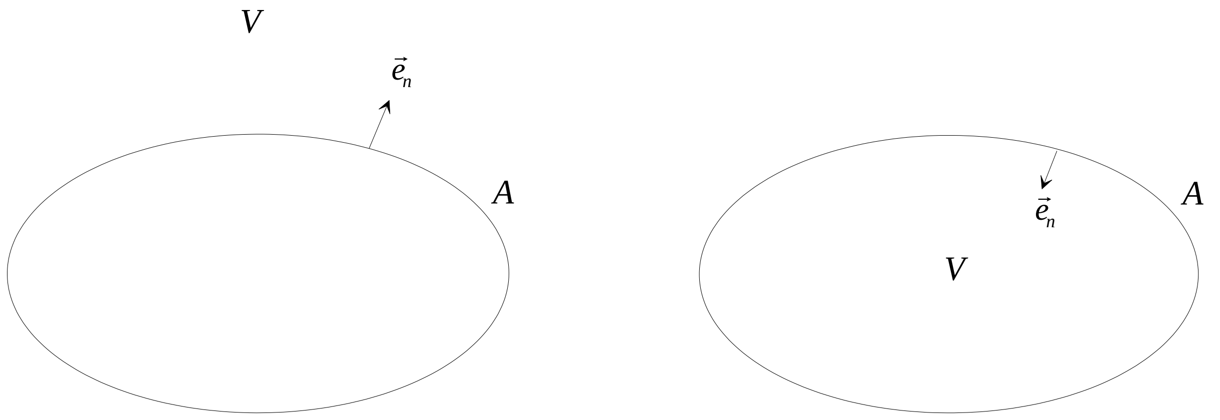

Figure 1. Fluid volume under consideration V, its closed boundary surface A and unit normal vector $\vec{e}_n$ at the boundary surface pointing towards volume V. Left: exterior problem, right: interior problem.

In time-harmonic fields (time dependence $e^{j\omega t}$, j = imaginary unit, $\omega = 2\pi f$ = angular frequency, *f* = frequency), the sound pressure in *V* and at *A*, obeying Eq. (1), can be obtained from the Helmholtz-Huygens integral [6, without source terms]

$$h(\vec{r})p(\vec{r}) = \int_V \left(\mathrm{j}\omega\rho_0 q'(\vec{r}_0) g(\vec{r}\,|\,\vec{r}_0) + \vec{f}(\vec{r}_0)\nabla_0 \cdot g(\vec{r}\,|\,\vec{r}_0) \right) \mathrm{d}V$$
$$+ \oint_A \left(p(\vec{r}_0)\nabla_0 g(\vec{r}\,|\,\vec{r}_0)\cdot\vec{e}_n + \mathrm{j}\omega\rho_0 \vec{u}(\vec{r}_0)\cdot\vec{e}_n g(\vec{r}\,|\,\vec{r}_0) \right) \mathrm{d}A, \tag{2}$$

where $\vec{u}$ is the particle velocity, *g* is the Green's function, subscript "0" is connected to the "source coordinates" that are integrated by the volume and surface integrals, and

$$h(\vec{r}) = \begin{cases} 0 \text{ in } R^3 - V \\ \frac{1}{2} \text{ at } A \\ 1 \text{ in } V. \end{cases} \tag{3}$$

On unsmooth surface points at *A*, the factor ½ in Eq. (3) has to be replaced by $\Omega / (4\pi)$ where Ω is the local space angle seen by the point towards the field region *V* [7].

The normal component of the particle velocity at *A* can be obtained also from the normal component of the pressure gradient as

$$\mathrm{j}\omega\rho_0 \vec{u}(\vec{r}_0)\cdot\vec{e}_n = -\nabla_0 p(\vec{r}_0)\cdot\vec{e}_n. \tag{4}$$

The three-dimensional Green's function in time harmonic fields and in free space is

$$g(\vec{r}|\vec{r}_0) = \frac{e^{-\mathrm{j}k|\vec{r}-\vec{r}_0|}}{4\pi|\vec{r}-\vec{r}_0|}, \tag{5}$$

where $k = \omega / c_0$ is the wave number.

So the sound pressure in the volume under consideration can be obtained from the Helmholtz-Huygens integral (2) if the source distributions in the volume and the field distributions on the boundary surface(s) are known. In the exterior problem the volume is outside the surface and in the interior problem it is inside the surface.

This approach is also often called “direct boundary integral formulation”. Acoustic problems which involve an open boundary surface are normally treated with the “indirect boundary integral formulation” [8].

4.2 Strong and weak problem formulation and the Galerkin method

In a strong problem formulation, one seeks a solution to a problem based directly on its field equation and pertinent boundary conditions. The solution has to obey the equations in all points of the medium and its boundaries. The problem can also be presented in a weak form if the field equation and the boundary conditions are required only to be fulfilled in a “average sense”, taking an integral as a starting point including implicitly the field equation and the boundary conditions in it [9]. This can be realized, e.g., with the variation methods or the moment methods.

In the variation methods, a proper functional is first produced, based on the field equation and the boundary conditions, and the solution is sought at its stationary value by varying the functional [10]. In Rayleigh-Ritz method, being a special case of the variation methods, the field is tried to be presented using known basis functions, and the error in the field approximation is orthogonal to the space spanned by these basis functions.

In the moment methods (weighted residual method, generalized Galerkin method) [11], the differential or integral field equation is treated directly. The field is approximated using predefined basis functions. The residual of the field equation is defined as its error in the map space. In addition to the basis functions, a set of testing functions (weighting functions) are selected and it is required that the residual is orthogonal with each of the testing functions, i.e., their inner products with the residual disappear. Typically, inner product on a surface is an area integral and in 3D space a volume integral.

The moment methods are divided into sub-methods based on the selection of the testing functions. In the Galerkin method, the testing function set is the same as the basis function set [11, 12]. Other moment methods are, e.g., the method of least squares, the collocation method and the subdomain method [12].

4.3 FEM and BEM

If in weak forms one uses piecewise continuous basis functions which are each non-zero inside some sub-region (element) (several functions can affect inside the same sub-region), and a node point inside or at the boundary of a sub-region is selected to present each of the basis functions, and the basis functions are demanded to fulfil the next terms

- at the node the values of all basis functions are zero, except the value of the basis function presenting the node is one
- the sum of basis functions at an arbitrary point in an element is one,

then the weak formulation is called the Finite Element Method (FEM) [13]. FEM is normally based on the differential field equations.

The Boundary Element Method (BEM) is a weak formulation where the basis functions are selected similarly as in FEM. However, the actual computation region is composed of the boundaries and the starting point is the Helmholtz-Huygens integral (2) instead of the differential equation of the field. When the field distributions on the boundary surface(s) have been calculated, the sound pressure can be calculated in selected points of the space using the same integral. The method is used for calculating diffracted fields and fields due to surface source distributions, in exterior and interior problems. The method is best applicable to exterior problems.

In calculating diffracted fields, the effects of the source distributions, situated inside the volume, are typically calculated separately with the free space Green's function as an incident field to the boundary surface, and then the diffracted field at the surface is calculated so that the total field meets the weak formulation of the Helmholtz-Huygens integral on the surface.

In exterior problems, BEM does not lead to a unique solution at frequencies corresponding the eigenfrequencies of the inner problem. Two mostly used methods to avoid this problem is the Burton–Miller integral equation (BMIE) [14] and the Combined Helmholtz Integral Equation Formulation (CHIEF) [15]. In the former, the traditional Helmholtz-Huygens integral equation is combined with its normal derivative. In the latter, some non-regularly situated node points are selected inside the surface and the sound pressure is put to zero value there.

There are some shortcomings in BEM models compared to coupled vibro-acoustic FEM models. The vibrational behaviour of boundary structures cannot be taken into account using their vibration equations, only boundary conditions (impedance) for acoustic fields can be associated to the boundary structures. Furthermore, the boundary conditions are given as locally reacting, in which case the velocity of one point is only associated to the sound pressure of the same point. Also different kinds of joints and stiffeners are difficult to be taken into account with BEM models. Further, sound transmission through structures and between structures cannot be taken into account with BEM. So, a true fluid-structure interaction and propagating waves in structures cannot be modelled only using BEM.

4.4 Mathematical background of CompA algorithm

4.4.1 General

CompA is based on BEM for solving the acoustic wave equation (time harmonic acoustic scattering) in 3D [2]. BEM is mostly used and best applicable to exterior problems and in this context it is used to interior problems where it is not as efficient as FEM. No computations in time domain are possible.

The incident fields are assumed to be generated by point sources and they are calculated using Green's function with real-valued wave number [2]. In the current version, the strengths of the point sources cannot be complex, to take their different phases into account, but this will be included in coming updates [4].

Internal losses of air can be taken into account by using complex sound velocity or complex wave number. The version that is currently used in Waveller Cloud uses real-valued wavenumber only but Kuava Oy has a newer version of the BE code which allows complex wave numbers [4].

Losses near boundaries (in small cavities) can be taken into account by hybrid FE-BE method where linearized Navier-Stokes equations are solved with FEM used near boundaries and the FEM mesh is truncated with BEM [16,2]. This is not implemented in the software, it has just tested using one-way coupling to Elmer LinNS FEM [4].

CompA algorithm uses BMIE for avoiding the non-uniqueness in exterior problems [2]. BMIE is stable also for interior problems [4].

CompA uses notation $e^{-i\omega t}$ for time harmonic dependence while in this report notation $e^{+j\omega t}$ is used. The correspondence is obtained if a notation i = – j is accepted.

4.4.2 Weakly singular weak form of BMIE

CompA uses the weakly singular weak form of BMIE [2]. The software uses first, second or third order polynomials as the basis and testing functions. The derivatives of the hypersingular integral operator are transformed into differentiable testing and basis functions. The singularity extraction technique is used to extract the singular terms from the kernel and they are integrated analytically. This is possible because flat triangular elements are used.

4.4.3 Solver algorithms

There are two possible solver algorithms. In algorithm 1, Gaussian elimination method as a direct solver is used. In algorithm 2, iterative GMRES is used with nearby groups and the fast broadband MLFMA is used with non-nearby groups [3].

The traditional solution methods (direct solvers) require $O(N^3)$ CPU time and $O(N^2)$ computer memory [2].

4.4.4 GMRES

The iterative methods require typically $N_{iter}O(N^2)$ CPU time and $O(N^2)$ computer memory. Computationally, the most expensive part is repeatedly done system matrix-vector product, especially with dense system matrix. The system matrix is complex and non-symmetric [2]. That is why the generalized minimal residual method (GMRES) [17] is used to solve the system iteratively [2]. It is suitable for numeric solution of non-symmetric system of linear equations [18].

With GMRES, for equation

$$Lf = g \, , \tag{6}$$

where L is a linear operator, the solution f is sought in Krylov subspace with minimum residual [18], Krylov subspace K_r of order r being [19]

$$K_r = \mathrm{span}\{g, Lg, L^2 g, \ldots, L^{r-1} g\} \, . \tag{7}$$

Arnoldi iteration [20] is used to find orthonormal vectors to Krylov subspace [18].

Before using GMRES, an incomplete LU preconditioner [21] is built to reduce the condition number of the problem so that the problem is more suitable for numerical solution. First the nearby terms in system matrix, corresponding to topologically close nodes, are picked, to form the matrix structurally symmetric and sparse. Next permutation matrix, obtained with Sloan algorithm [22, 23], is applied to minimize the fill-in of the LU decomposition [2]. In the software, a threshold parameter τ defines the values that are left to incomplete LU, the smaller the value, the more entries is put in the preconditioner. This is comparable to droptol-parameter in Matlab's ILU-function. A negative value of τ causes the problem to be solved without the preconditioner [4].

4.4.5 FMM and MLFMA

In the fast multipole method (FMM) [24, 25], the unknowns are divided into groups by their location in space. Fields of each group are combined. Only contributions of neighbouring groups are calculated by traditional way (here with GMRES). Contributions of groups far from each other are calculated via an approximate fast scheme. Outgoing total field of each group is presented as a far field pattern. Interaction between non-nearby groups are formulated using Rokhlin's translation formula [24], giving local plane wave expansion at receiving group and translating far field pattern into near field pattern. Fields at each element in groups are computed from the plane wave expansion. Computational cost is $O(N^{3/2})$.

In the multilevel fast multipole algorithm (MLFMA) [26, 25], several grouping levels in a tree-like structure. First the object is enclosed into a large cube at level 0. Then the cube is recursively divided into eight cubes at following levels. The number of levels is selected so that the smallest group size is about $\lambda/4$, where λ is the wavelength. The algorithm requires $N_{\text{iter}}O(N\log N)$ CPU time and $O(N)$ computer memory [2].

As drawbacks in FMM and MLFMA, there occurs a sub-wavelength breakdown (low frequency breakdown) when the size of the groups becomes small compared to wavelength [24]. So the algorithms cannot be used at low frequencies. Furthermore, the numerical approximation error cannot be reduced beyond a certain limit. The methods diverge as the number of unknowns per group is increased beyond a certain threshold and they cannot be used if the discretization of geometry includes small details compared to wavelength or when high accuracy is required [2].

For those reasons, the broadband MLFMA is used where the translation function of FMM (Rokhlin's translation function) is replaced with a spectral representation of Green's function (inhomogeneous plane wave expansion) for small group sizes [27, 28, 29, 30, 31, 32]. This makes versatile mesh refinements possible. As a drawback, the method is direction dependent and it requires six times more memory than the traditional MLFMA. That is why the Rokhlin's translation function is used for large group sizes (i.e, > $\lambda/2$) [2]. In the program, the limit size is chosen automatically [4].

5. Use case of acoustic simulation

The case study is concentrated on the sound field distributions produced by an acoustic point source into the interior of a tractor cabin, and simulation of material utilization in the inner roof element. Valtra cabin T888M is used as a test case because calculated results exist for that based on FEM simulations in NOVI project [33], making it possible to compare the BEM results of this project to the results of NOVI. Three inner roof elements, used in NOVI project, were selected for that purpose.

With Waveller Cloud, Matlab-interfaces are used for putting the input data in a proper format and for presenting the computation results [1]. Some preliminary steps have been taken and some extra Matlab functions have been created to get all pertinent input data into the computations in the format needed. Also the Matlab-interface for input data has been modified to use these new Matlab functions.

5.1 Definition of the impedance of surface elements

The impedance data of roof, window and wall elements, needed in the computation, are calculated with NOVA program of ESI Group. A Matlab function "readz.m" has been created to read impedance data from NOVA output and revising it to the Matlab-interface. First the proper impedance data Z

$$Z = -\frac{p}{\vec{u}\cdot\vec{e}_n} \tag{8}$$

is read from a file, then it is scaled to normalized impedance z by

$$z = \frac{Z}{\rho_0 c_0} \tag{9}$$

and finally, if necessary, interpolated to frequencies used in the Matlab-interface. The negative sign in Eq. (8) is due to that the impedance is defined by the normal velocity component towards the surface from volume *V* and the unit normal vector has an opposite direction.

The surface impedances, calculated with NOVA, do not take into account the lateral dimensions of the structures but it is assumed that the specimens are part of laterally infinite structures.

5.1.1 Three inner roof elements

The inner roof construction used in the simulations is presented in Figure 2. The material constants are presented in Table 1 and Table 2.

Table 1. Material constants of fluid phases.

	Absorbent fluid phase	Inner roof 2 fluid phase	Inner roof 3 fluid phase
Density [kg/m^3]	1.225	1.225	1.225
Sound speed [m/s]	287.6	287.6	287.6
Porosity	0.95	0.95	0.95
Flow resistivity [Pas/m^2]	75 000	75 000	35 000
Tortuosity	1.1	1.1	1.1
Viscous characteristic length [µm]	44	44	44
Thermal characteristic length [µm]	63	63	63

Table 2. Material constants of solid phases.

	Absorbent solid phase	Inner roof 1	Inner roof 2/3 solid phase	Windows	Steel body elements
Thickness [mm]	50	6	6	5	3
Density [kg/m^3]	88.8	316.5	14	2 500	7 800
Young's modulus [MPa]	0.3333	75	75	60 000	210 000
Poisson's ratio	0.3	0.2	0.3	0.23	0.31
Damping loss factor	0.01	0	0	0.02	0.001

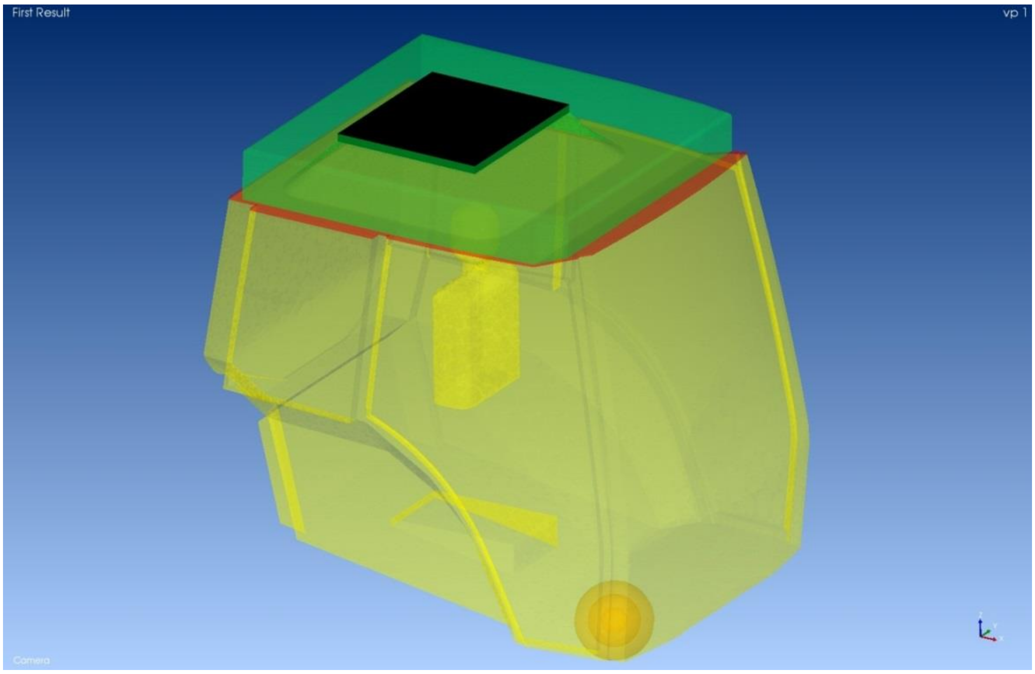

Figure 2. Valtra cabin T888M used in simulations. Inner roof centre part has a 50 mm thick absorbent above (dark green) and outer part has a 194.2 mm thick air gap (light green) back of it below the steel body.

The surface impedances of the inner roof structures, calculated with NOVA, are presented in Figure 3, Figure 5 and Figure 7 at frequencies 80 – 400 Hz, and in Figure 4, Figure 6 and Figure 8 at frequencies 20 – 2000 Hz.

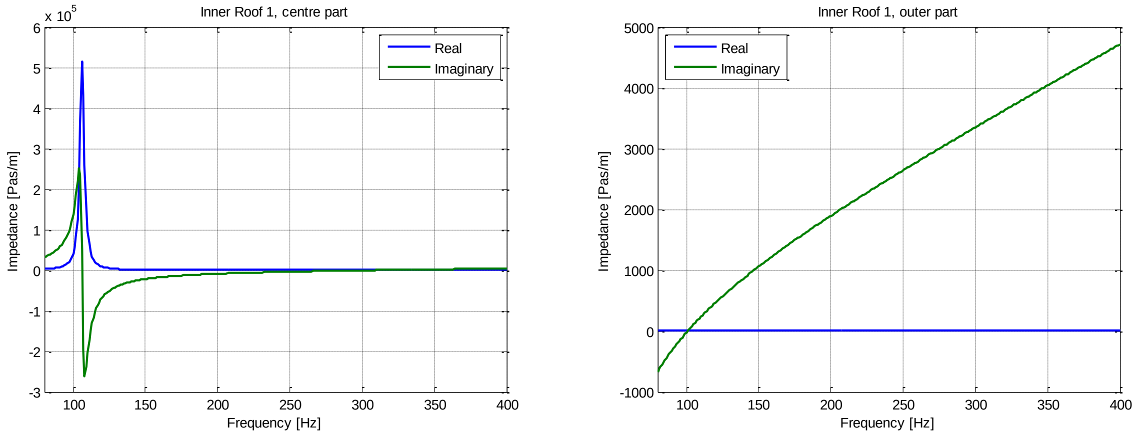

Figure 3. Calculated surface impedance of inner roof 1 at frequencies 80 – 400 Hz.

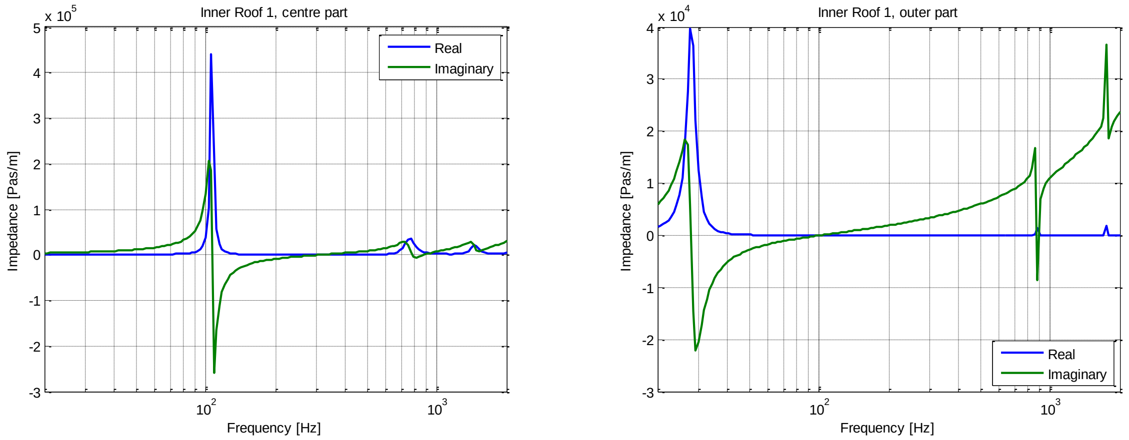

Figure 4. Calculated surface impedance of inner roof 1 at frequencies 20 – 2000 Hz.

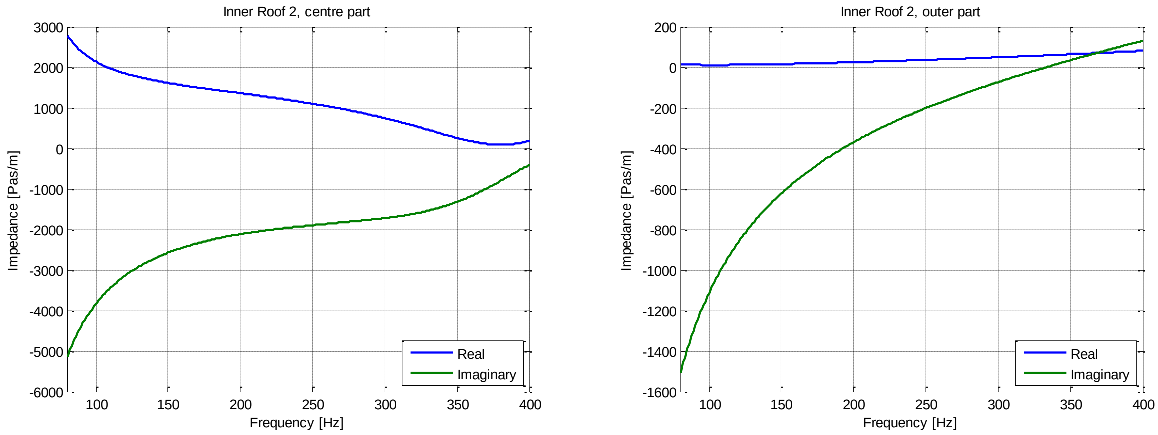

Figure 5. Calculated surface impedance of inner roof 2 at frequencies 80 – 400 Hz.

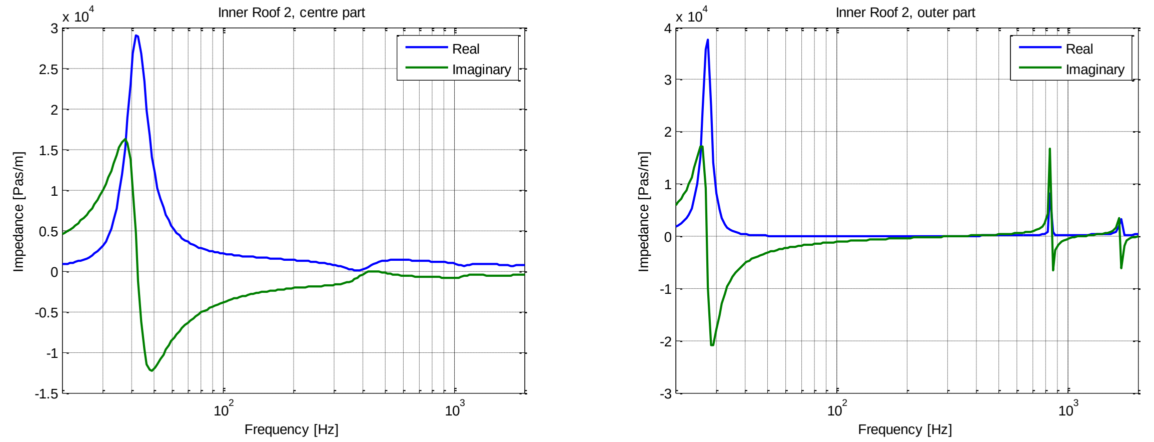

Figure 6. Calculated surface impedance of inner roof 2 at frequencies 20 – 2000 Hz.

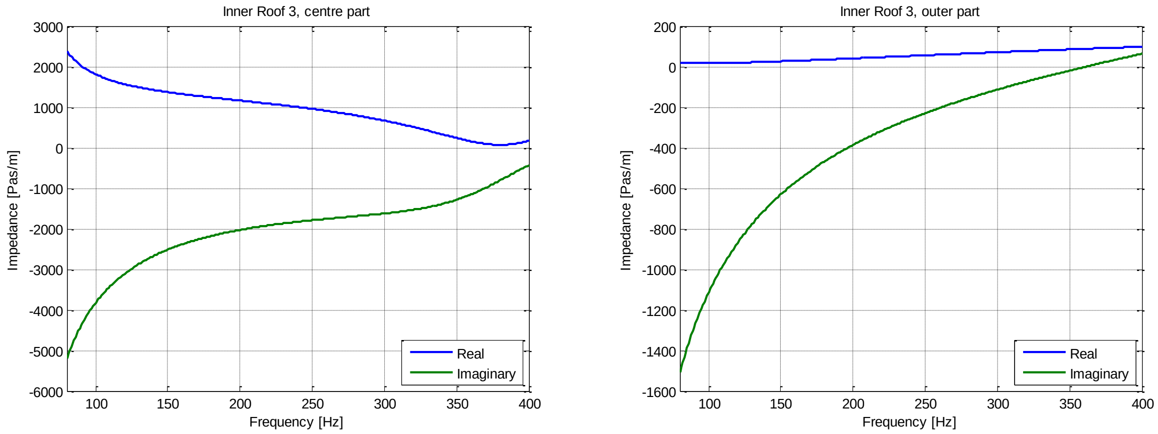

Figure 7. Calculated surface impedance of inner roof 3 at frequencies 80 – 400 Hz.

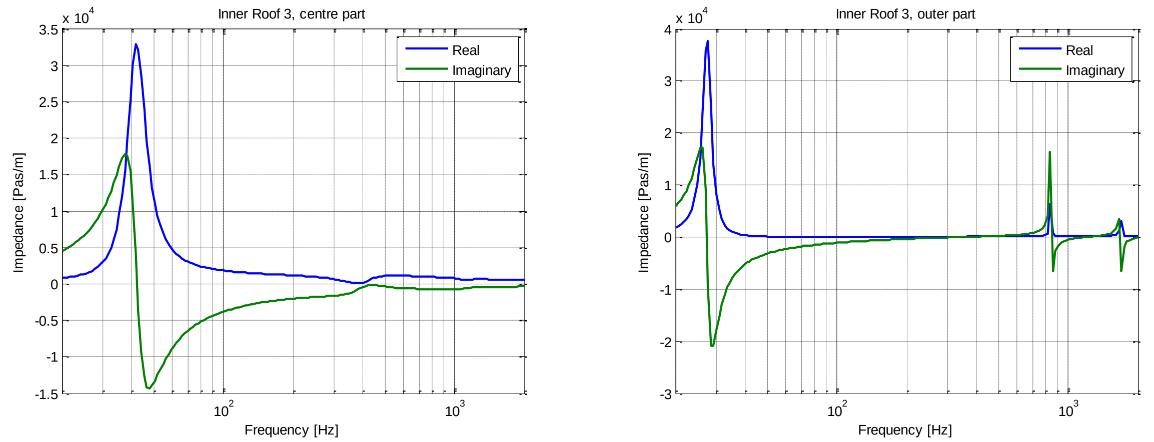

Figure 8. Calculated surface impedance of inner roof 3 at frequencies 20 – 2000 Hz.

5.1.2 Other interior surfaces

The walls and windows have been modelled as isotropic solids. The walls are made of steel with 3 mm thickness and other parameters as follows: Young's modulus 210 GPa, density 7800 kg/m^3, Poisson's ratio 0.31 and loss factor 0.001. The windows are 5 mm thick and other parameters as follows: Young's modulus 60 GPa, density 2500 kg/m^3, Poisson's ratio 0.23 and loss factor 0.02.

The calculated impedance data for wall and window elements is presented in Figure 9 at frequencies 80 – 400 Hz, and in Figure 10 at frequencies 20 – 2000 Hz.

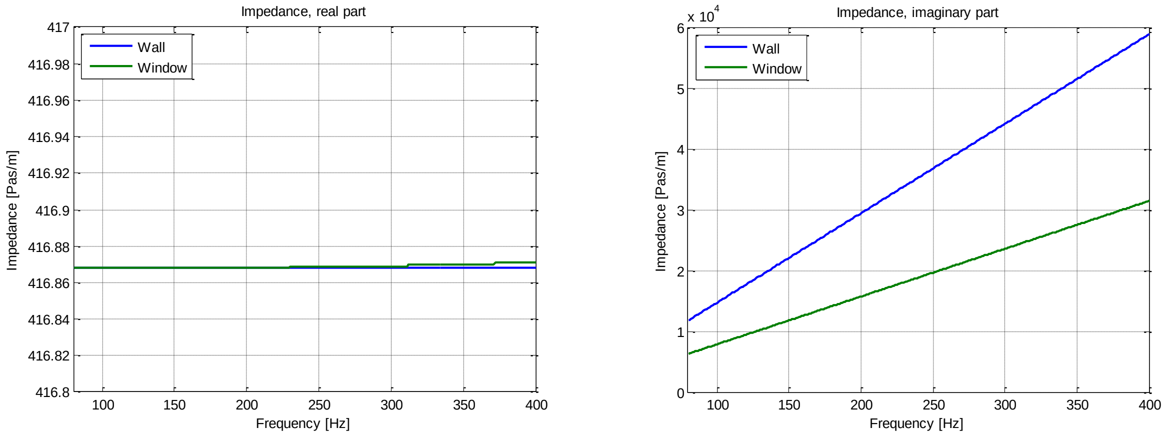

Figure 9. Wall and window surface impedances at frequencies 80 – 400 Hz.

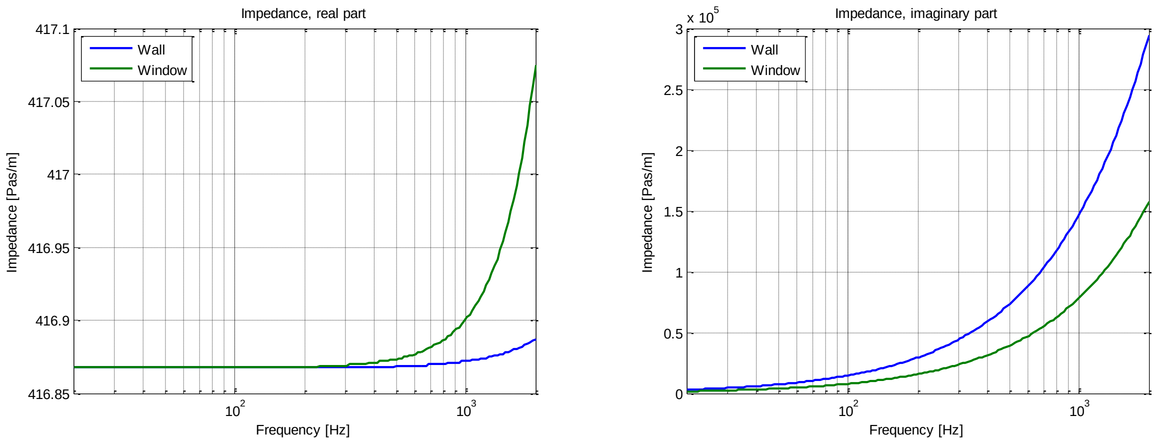

Figure 10. Wall and window surface impedances at frequencies 20 – 2000 Hz.

5.2 Modifications in Matlab-interface for input

5.2.1 Converting impedance and velocity data to boundary condition parameters

Three types of element-wise boundary conditions, used typically in FEM and BEM programs, Dirichlet boundary condition, Neumann boundary condition and impedance boundary condition, can be used [2]. Also a velocity boundary condition may be used.

The boundary condition is given by parameters *a*, *b* and *c* so that

$$ap + b\nabla p \cdot \vec{e}_n = c\,. \tag{10}$$

The Neumann boundary condition (sound hard body, infinite impedance, normal component of the particle velocity vanishes) is obtained by selecting $a = 0$, $b = 1$ and $c = 0$. This is the default value given by the Matlab-interface unless otherwise selected.

The Dirichlet boundary condition (sound soft body, zero impedance, sound pressure vanishes) is obtained by selecting $a = 1$, $b = 0$ and $c = 0$.

The normalized impedance of the boundary can be given, by the help of Eqs. (9), (8) and (4) as

$$z = -\frac{1}{\rho_0 c_0}\frac{p}{\vec{u}\cdot\vec{e}_n} = \frac{\mathrm{j}\omega}{c_0}\frac{p}{\nabla p\cdot\vec{e}_n}\,. \tag{11}$$

Now the impedance boundary condition is obtained by selecting *b* = 1, *c* = 0 and

$$a = -\mathrm{j}\frac{\omega}{c_0 z}\,. \tag{12}$$

A Matlab function ”impbc.m” has been created to give these boundary condition parameters of the impedance boundary for the Matlab-interface. Also a Matlab function “bcsz.m” has been created to convert these parameters to the boundary condition data set BCS in the Matlab-interface. As stated in Section 5.1, A Matlab function “readz.m” has been created to read impedance data from NOVA output and revising it to the Matlab-interface for further handling to the boundary condition data. The Matlab-interface for input has been modified to use these new Matlab functions in formatting the necessary surface impedance data for Waveller Cloud.

A velocity boundary condition can be obtained by selecting *a* = 0, *b* = 1 and, by the help of Eq. (4),

$$c = -\mathrm{j}\,\omega\rho_0\vec{u}\cdot\vec{e}_n\,. \tag{13}$$

A Matlab function “velbc.m” has been created to give these boundary condition parameters of the boundary with predefined velocity distribution. This Matlab function has not been used in the simulations.

5.3 Simulating acoustic fields

5.3.1 Scaling the source strengths

The sound pressure *p* of a time harmonic point source in a free space at a distance *r* from the source is expressed in CompA algorithm as

$$p = \frac{C}{4\pi}\frac{\mathrm{e}^{\mathrm{i}kr}}{r}\,, \tag{14}$$

where *C* is called as the magnitude of the source [2]. The same expression in the logic of Actran is

$$p = A\frac{\mathrm{e}^{-\mathrm{i}kr}}{r}\,, \tag{15}$$

where *A* is called as the amplitude of the source [34]. The value of *C* is given as the source strength in Waveller Cloud and the value of *A* in Actran. In both simulations the source strength was set as 1 which gives a difference of 4π. This was compensated in the results of Waveller Cloud by multiplying the pressure values by 4π, to get the results comparable. In dB scale, this corresponds adding 22 dB to the results. The difference in the signs of the imaginary units in Eqs. (14) and (15) is due to different time harmonic notations, see Section 4.4.1.

5.3.2 Sound field distributions

A torso was included in the interior of the cabin, to simulate the effects of the head and chest of the driver, see Figure 2. The Cartesian coordinate system for the model was such that the *x*-coordinate axis goes in the longitudinal direction from the back of the cabin towards the front part, the *y*-coordinate axis goes in the transversal direction from the right side to the left side of the cabin (as looked by the torso), and the *z*-coordinate axis goes in the upward direction from the bottom of the cabin towards the roof, as presented in Figure 2.

The sound pressure level distributions were calculated at frequency range 80 – 400 Hz with the resolution of 1 Hz at three orthogonal cross-sectional planes in the cabin. The first plane was at x = – 0.2889 m (just before the torso), the second plane was at y = 0 m (longitudinal vertical cross section going through the middle of the torso), and the third plane was at z = 0.8007 m (horizontal cross section going through the torso below its head). The source point was at x = 0.40823817 m, y = – 0.49747461 m and z = 0.095712125 m, at the front right bottom corner of the cabin.

5.3.3 Sound field distributions at 100 Hz

The sound pressure level distributions at 100 Hz at the three orthogonal cross-sectional planes in the cabin, computed with Actran and Waveller Cloud, are presented in Figure 11 for the inner roof 1, in Figure 12 for inner roof 2, and in Figure 13 for inner roof 3. In the first plane the corresponding figures are looking from the front of the cabin and in the third plane the corresponding figures are looking from the roof of the cabin.

The distributions and absolute levels for the inner roof case 1, computed by Actran and Waveller Cloud, deviate a lot. This deviation is probably mostly due to the plate resonance in the surface impedance of the outer part of the inner roof 1 and the antiresonance in the surface impedance of the centre part of the inner roof 1, both occuring near 100 Hz. The plate resonance frequency f_p can be calculated by equation

$$f_p = \frac{c_0}{2\pi}\sqrt{\frac{\rho_0}{\rho_s dD}} = 98.7\ \text{Hz}, \tag{16}$$

where ρ_s and d are the density and thickness of the plate (inner roof material) and D is the thickness of the air volume behind the plate (194.2 mm, outer part of the inner roof). The antiresonance of the centre part of inner roof 1 can be seen in Figure 3 or better in Figure 15. The antiresonance is characterized by a maximum value of the magnitude of the impedance together with a 180° drop in the phase of the impedance.

The phenomenon is only due to the logic where the centre and outer parts of the inner roof are treated separately. In reality, the inner roof parts are strongly structurally and acoustically coupled and they act as one entity, and the apparent resonance and antiresonance do not affect independently but are rather coupled to some combined behaviour. The strong coupling of the inner roof centre and outer parts cannot be taken into account by BEM methods because the roof parts are only treated as separate surface impedances. Treating strongly coupled near-by surfaces as separate may generally lead to erroneous results in BEM computations if the individual surface properties deviate much from each other. At least in this kind of situation, the near-by surfaces should be treated as one entity having a non-locally reacting surface impedance as a function of spatial coordinates. Non-locally reacting surface means a surface where the velocity of one point on it depends on the sound pressure at every point on the surface, leading to surface impedance matrices, including driving point impedances and transfer impedances. Admittances, i.e., mobilities are rather used in that case, the admittance matrix being the inverse of the impedance matrix, see, e.g., [9]. This kind of matrices could be computed by FEM but then we do not talk about a pure BEM model any more.

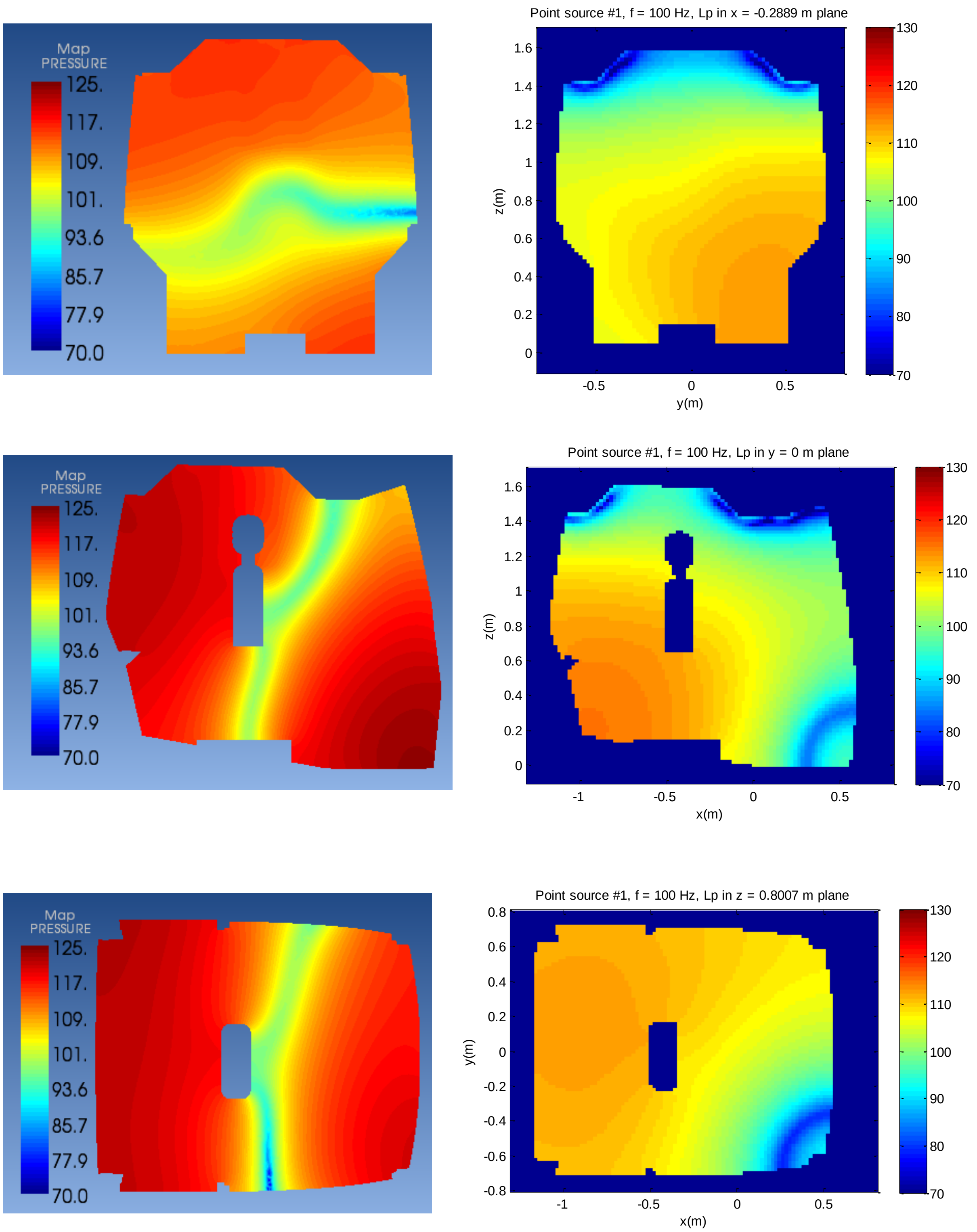

Figure 11. Sound pressure level distributions at three surfaces in the cabin at 100 Hz; left: Actran results, right: Waveller Cloud results; inner roof 1.

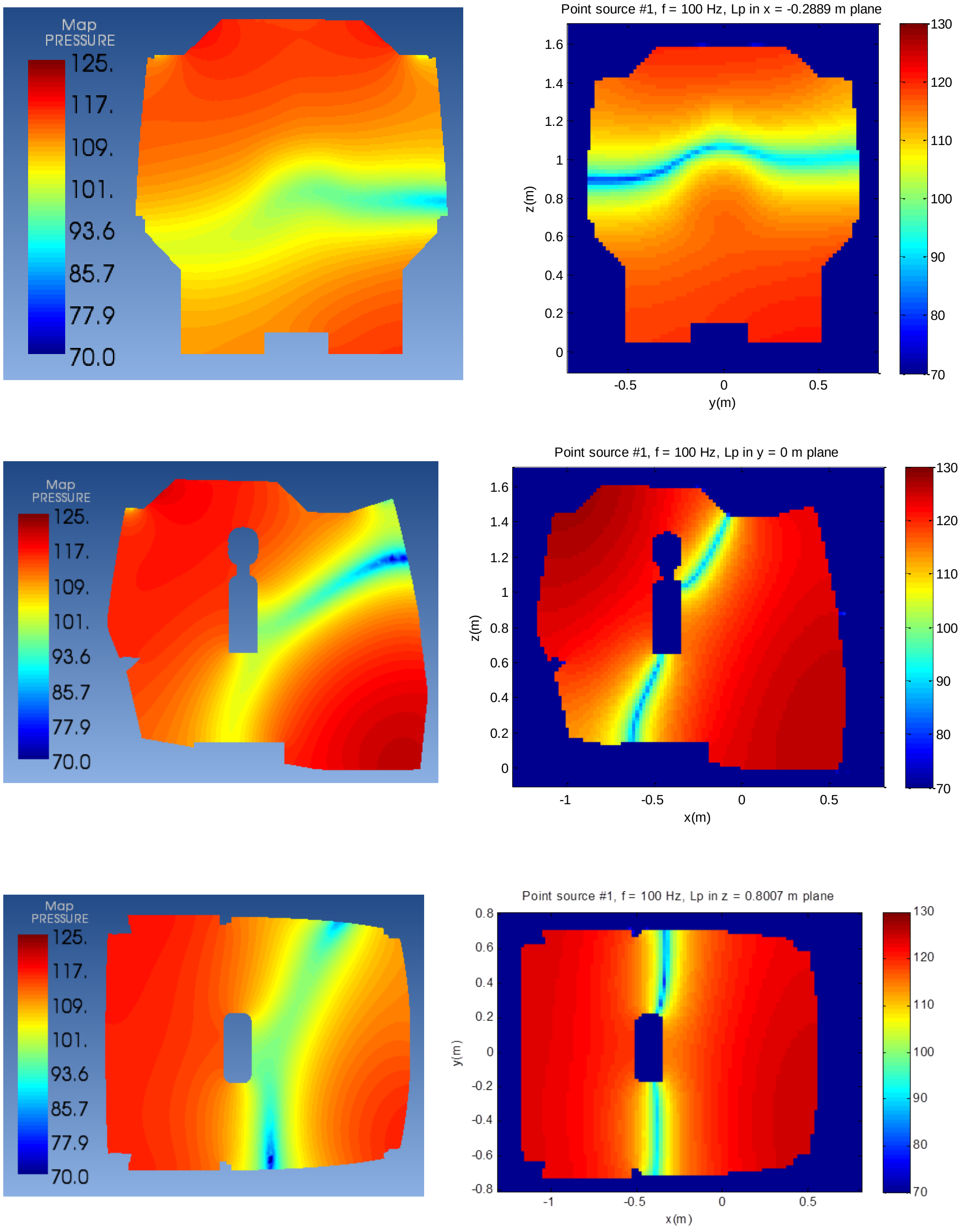

Figure 12. Sound pressure level distributions at three surfaces in the cabin at 100 Hz; left: Actran results, right: Waveller Cloud results; inner roof 2.

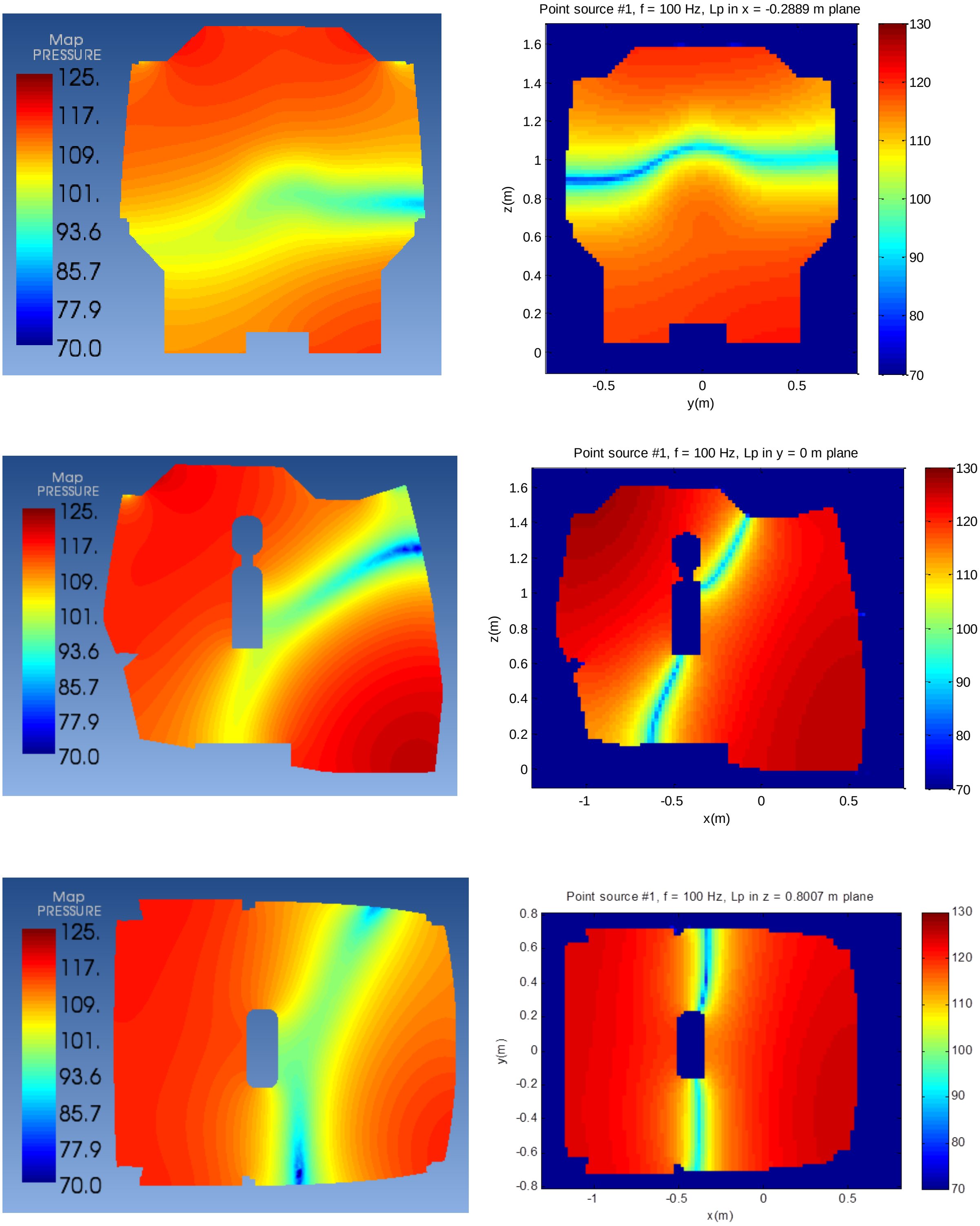

Figure 13. Sound pressure level distributions at three surfaces in the cabin at 100 Hz; left: Actran results, right: Waveller Cloud results; inner roof 3.

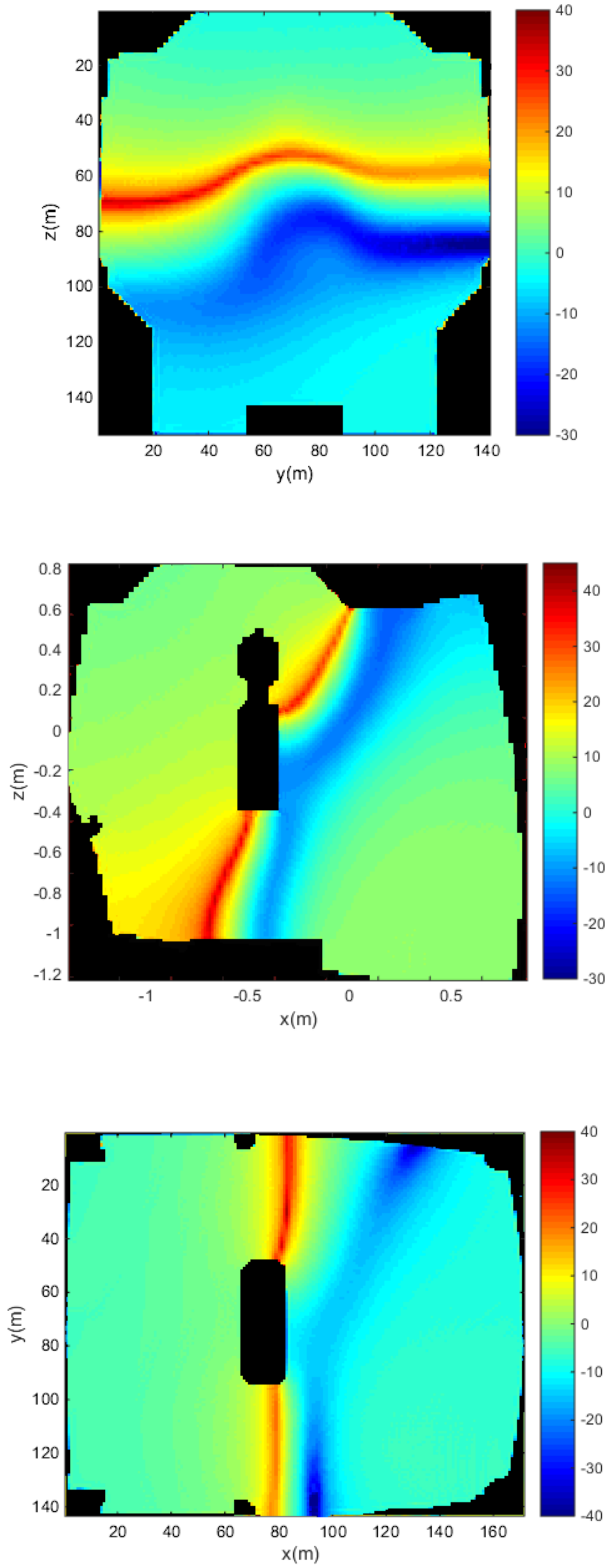

Figure 14. Difference in sound pressure level distributions (Actran results – Waveller Cloud results) at three surfaces (same as in previous figures) in the cabin at 100 Hz; inner roof 2.

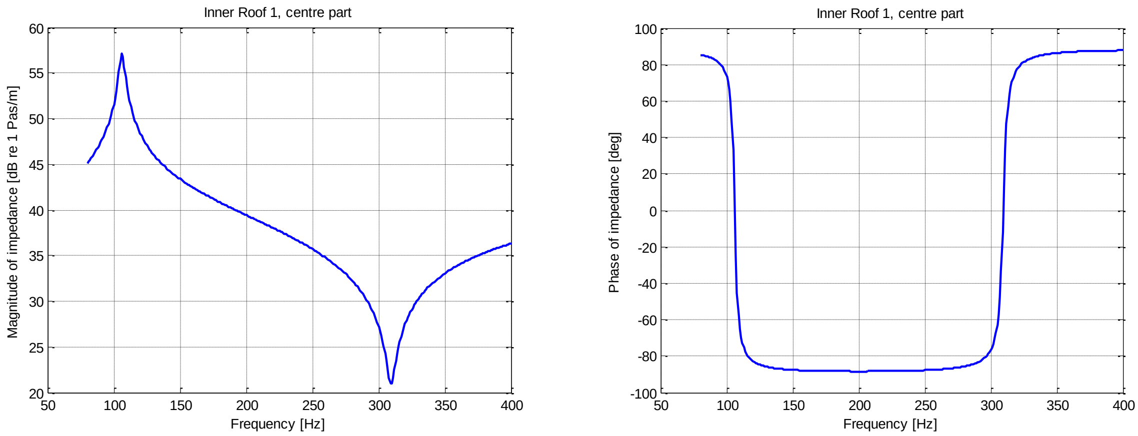

Figure 15. Magnitude and phase of the surface impedance of inner roof 1, centre part.

The surface impedances of the centre and outer parts of inner roofs 2 and 3 near 100 Hz are also different, as can be seen in Figure 5 and Figure 7. However, their dependence of frequency is much smoother. This probably leads to that the distributions and absolute levels for the inner roof cases 2 and 3 are quite near each other for both of the computations at 100 Hz. However, the small deviations in the proportional sound field distributions are probably due to treating the boundary surfaces as locally reacting in BEM. The difference in the sound pressure level distributions, presented for the inner roof case 2 in Figure 14, is due to the deviations in the proportional sound field distributions, mainly the minimum values occurring at a little different locations, so their actual values are not so significant in comparing the results of the different programs.

Waveller Cloud seems to give a little higher sound pressure levels than Actran. This is probably due to using complex sound velocity in the air space of the cabin, used with the Actran model, to take into account some dissipation effects, not taken into account in the structural parameters, and the effect of sound transmission outwards through the structure. The value of the imaginary part of the sound velocity was based on reverberation time measurements inside the cabin. With the current version of Waveller Cloud, complex sound velocity cannot be used. This leads to weaker internal losses and higher sound pressure levels.

6. End-user experience of the Waveller Cloud computation environment

6.1 Modelling chain

6.1.1 Pre-processing

Before the actual computation, some pre-processing steps are needed, in addition to the definition of the impedances of the surface elements as presented in Section 5.1.

From the STEP-formant CAD geometry of the simulated cabin, a numeric mesh definition file as a Matlab dat-file has to be created as stated in Ref. [3]. It should contain the surface mesh of the cabin with node and element definitions in format which is compatible with Waveller Cloud. This file contains the locations of all nodes of the surface mesh and node indexes of the nodes belonging to each element. Also a mat-file for indicating which surface elements belongs to which surface impedance category has to be created. This file is not needed in Waveller Cloud but it is needed in the modified Matlab-interface to produce the boundary condition data proper for Waveller Cloud [3] in the way as stated in Section 5.2.1.

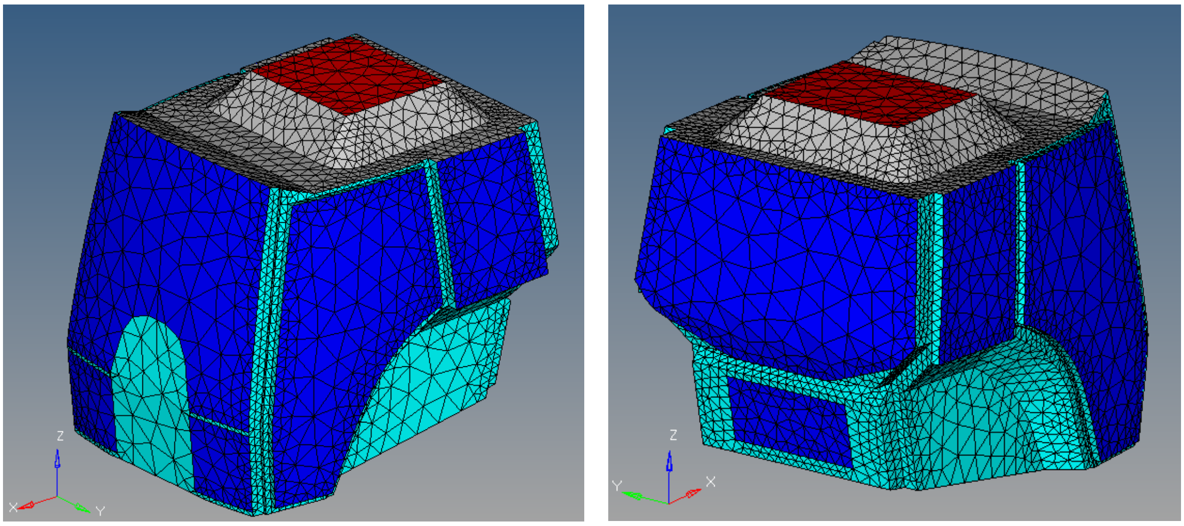

Figure 16. Surface mesh of the modelled cabin with different impedance boundary conditions. Cyan: body, blue: windows, grey: inner roof, red: inner roof backed with wool.

All other input is given in the Matlab interface. Especially, the source points and the sound pressure computation points have to be given numerically in the Matlab files. From the required files and other input data, actual input data for computation in Waveller Cloud is made using the Matlab interface script. This Matlab script creates relevant input data for every frequency calculated in the simulation. All of these files of the input data are then archived into a zip file. This zip file is uploaded into server where the actual computation with Waveller Cloud is made [1].

Using Matlab as the main tool for creating input data for computation is very flexible but it may also introduce some challenges. One needs to have acquired at least basic skills in Matlab coding in order to understand or modify the code which is written to produce the input data for computation. It is also important to note that not every company have purchased this program nor necessarily have acquired sufficient skill to use it. Another difficulty is the need of producing the extra files, namely the mesh definition file, the surface impedance category file and the surface impedance files, before using the actual Matlab interface. In this project, these files have been generated with NOVA program but every company does not have suitable tools for surface impedance definitions. Some auxiliary program is needed for the surface impedance definitions, especially when the structure contains absorptive elements, as is the case here.

It was found out that creating input the files for every calculated frequency could lead in some cases to incorrect file names (see Figure 17). This is the case when desired computation frequency is not an integer. For example, if desired computation frequencies are 100 Hz and 100.1 Hz, they are both renamed in the input file process as fieldPressurePointSource1Freq0100Hz.dat.

fieldPressurePointSource1Freq0400Hz.dat	19.12.2013 10:30	DAT File	1 498 KB
fieldPressurePointSource1Freq0399Hz.dat	19.12.2013 10:27	DAT File	1 498 KB
fieldPressurePointSource1Freq0398Hz.dat	19.12.2013 10:25	DAT File	1 498 KB
fieldPressurePointSource1Freq0397Hz.dat	19.12.2013 10:23	DAT File	1 499 KB
fieldPressurePointSource1Freq0396Hz.dat	19.12.2013 10:21	DAT File	1 499 KB
fieldPressurePointSource1Freq0395Hz.dat	19.12.2013 10:18	DAT File	1 499 KB

Figure 17. Some input files for computation. Note only integer numbers in frequency information in name files.

It would be more convenient to have better compatibility with different mesh types. In fact, there could be a possibility to upload a mesh in Waveller Cloud environment where actual conversion to Waveller-compatible mesh is automatically made.

6.1.2 Computation

The computation itself was quite straightforward. There were no errors during simulations. Computation time was about 8 h 20 min. In contrast, computation time was 4 h 11 min in one of VTT's workstation.

	Kuava (MLFMA)	**VTT (FEM)**
processor	Intel Xeon X3363 @ 2.83GHz	Intel Xeon X5690 @ 3.47 GHz
number of processors	4	8
operation system	Red Hat Enterprise Linux Server release 5.4 (Tikanga) 64-bit	linux-libc234-x86-64
RAM used	0.5 GB	6 GB
computation time	8 h 20 min	4 h 11 min

6.1.3 Post-processing

The results of Waveller Cloud are given in a zipped package [1]. The post-processing is done with a Matlab interface, as is the case with the pre-processing. Any changes in the way of printing the results need changes in the Matlab script. So the remarks considering the flexibility and challenging aspects with the Matlab input interface also apply to the Matlab post-processing interface.

6.2 Waveller Cloud web interface

In this project, Waveller Cloud web interface was used in Microsoft Windows 7 environment with Mozilla Firefox 27.0 web browser. In order to get access to Waveller Cloud, user needs to have static IP- (internet protocol) address and account to use Waveller Cloud. The motivation and need of requiring Static IP-address is unclear and it seems it is unnecessary. It seems that this only a temporary precaution because of the state of the calculation environment.

For the preparation of the computation, simulation package file is uploaded to the server. The job queue will display the status of this and all the previous simulations by the user. Job queue is implemented by Kuava. If the status is “initialized”, then this simulation is ready for execution. In order to start the actual computation of the simulation case, the user needs to click “initialized” status of the current simulation case and, in a new window, press “solve (selected)” button. This is a somewhat confusing and unnecessary step. After uploading the simulation file and checking whether the simulation file is valid (initialized state), there could be something like “run all frequencies” and “run selected frequencies” buttons in the queue list.

When the computation is finished, the results can be downloaded. Also, new frequencies can be appended to this simulation to extend the simulation frequencies used in the computation. This is a very good and helpful option.

7. Conclusions

Acoustic simulation test case was performed with Kuava Oy's new software application Waveller Cloud (under development). The software is available for local as well as cloud computing.

First some basic theory behind the software was presented, containing the Helmholtz–Huygens integral, strong and weak problem formulations, the Galerkin method, and how the boundary element method, used in Kuava Oy's software with CompA algorithm, is bound to these concepts.

CompA is based on the boundary element method (BEM) for solving the acoustic wave equation (time harmonic acoustic scattering) in 3D. BEM is mostly used and best applicable to exterior problems and in this context it was used to interior problems where it is not as efficient as the finite element method (FEM).

In the current version of the program, the different phases of the sound sources cannot be taken into account, but this will be included in coming updates. Internal losses of air neither can be taken into account but Kuava Oy has a newer version of the BE code which removes this rejection.

CompA algorithm uses Burton–Miller integral equation (BMIE) for avoiding the non-uniqueness in exterior problems. BMIE is stable also for interior problems. CompA uses the weakly singular weak form of BMIE. The software uses first, second or third order polynomials as the basis and testing functions. The derivatives of the hypersingular integral operator are transformed into differentiable testing and basis functions. The singularity extraction technique is used to extract the singular terms from the kernel and they are integrated analytically. This is possible because flat triangular elements are used.

There are two possible solver algorithms. In algorithm 1, Gaussian elimination method as a direct solver is used. In algorithm 2, iterative generalized minimal residual method (GMRES) is used with nearby groups and the fast broadband multilevel fast multipole algorithm (MLFMA) is used with non-nearby groups.

There are some shortcomings in BEM models compared to coupled vibro-acoustic FEM models. The vibrational behaviour of boundary structures cannot be taken into account using their vibration equations, only boundary conditions (impedance) for acoustic fields can be associated to the boundary structures. Furthermore, the boundary conditions are given as locally reacting. Also different kinds of joints and stiffeners are difficult to be taken into account with BEM models. Further, sound transmission through structures and between structures cannot be taken into account with BEM. So, a true fluid-structure interaction and propagating waves in structures cannot be modelled only using BEM.

The case study was concentrated on the sound field distributions produced by an acoustic point source into the interior of a tractor cabin, and simulation of material utilization in the inner roof element. Valtra cabin T888M was used as a test case because calculated results exist for that based on FEM simulations in NOVI project, making it possible to compare the BEM results of this project to the results of NOVI. Three inner roof elements, used in NOVI project, were selected for that purpose. This comparison is not valid for all aspects because BEM and FEM models handle some affecting things in a different manner and some affecting things cannot be modelled or their modelling is not so straightforward in BEM. Especially, treating strongly structurally and acoustically coupled near-by surfaces as separate and locally reacting may generally lead to erroneous results in BEM computations if the individual surface properties and their frequency dependencies deviate much from each other. This is probably the main reason for the largely different results of the sound pressure levels and their proportional distributions in the cabin at 100 Hz with Actran and Waveller Cloud computations for the inner roof case 1 in Figure 11. In this kind of situation, the near-by surfaces should be treated as one entity having a non-locally reacting surface impedance matrix as a function of spatial coordinates. Also the small deviations in the proportional sound field distributions with FEM and BEM calculation results for the inner roof cases 2 and 3 in Figure 12 and Figure 13 are probably due to treating the boundary surfaces in different ways in FEM and BEM. Otherwise, the calculation results of Waveller Cloud and Actran for the inner roof cases 2 and 3, concerning the sound pressure distributions, are tolerably in agreement. One conclusion from the simulation results is that using BEM in interior problems is very sensitive to proper impedance definitions of the boundaries.

With Waveller Cloud, Matlab-interfaces are used for putting the input data in a proper format and for presenting the computation results. Before the actual computation, some pre-processing steps are needed to be made. From the mesh of the simulated cabin, a numeric mesh definition file has to be created, containing surface mesh of the cabin with node and element definitions in format which is compatible with Waveller Cloud. In addition, a file for indicating which surface elements belong to which surface impedance category has to be created. Furthermore, some preliminary steps have been taken and some extra Matlab functions have been created to get the surface impedance input data into the computations in the boundary condition format needed. The surface impedances of the surface elements were calculated with NOVA program and the impedance data was read to the Matlab interface by a new Matlab function. Further, two Matlab functions were created to give this impedance data to the boundary condition parameters, used in Waveller Cloud. The Matlab-interface for input has been modified to use these new Matlab functions.

Using Matlab as the main tool for creating input data for computation is very flexible but also quite challenging. One needs to have acquired at least basic skills in Matlab coding in order to understand or modify code which is written to produce input data for computation. Another difficulty is the need of producing the extra files for mesh definitions, surface impedance categories and surface impedance definitions, before using the actual Matlab-interface. Some auxiliary program, besides Matlab, is needed for the surface impedance definitions, especially when the structure contains absorptive elements, as is the case here.

8. Summary

Acoustic simulation test case was performed with Kuava Oy's software application Waveller Cloud. It uses CompA algorithm which is based on the boundary element method (BEM) for solving the acoustic wave equation in frequency domain. BEM is mostly used and best applicable to exterior problems and in this context it was used to interior problems where it is not as efficient as the finite element method (FEM). Furthermore, a true fluid-structure interaction and propagating waves in structures cannot be modelled only using BEM as they can with coupled vibro-acoustic FEM, only locally reacting boundary conditions (impedance) for acoustic fields can be associated to the boundary structures. This may cause errors with individual strongly coupled near-by surface parts especially if the individual surface properties deviate much from each other.

The case study, Valtra cabin T888M, was concentrated on the sound field distributions produced by an acoustic point source into the interior of a tractor cabin, and simulation of material utilization in three inner roof elements for which calculated results exist based on FEM simulations in NOVI project. Probably the main reason for the largely different results of the sound pressure level distributions in the cabin at 100 Hz of Waveller Cloud calculations, compared to those of Actran, for the inner roof case 1 is treating separately and as locally reacting the centre and outer parts of the inner roof. Also the small deviations in the sound field distributions for the inner roof cases 2 and 3 are probably due to the handling of some affecting things in a different manner in FEM and BEM models. Otherwise, these computed results are tolerably in agreement. Using BEM in interior problems is very sensitive to proper impedance definitions of the boundaries.

With Waveller Cloud, Matlab-interfaces are used for putting the input data in a proper format and for presenting the computation results. Using Matlab as the main tool for creating input data for computation is very flexible but also quite challenging. The Matlab-interface for input has been modified to use three new Matlab functions in reading the impedance data of the surface elements, calculated with NOVA, and formatting the data to the boundary condition parameters for Waveller Cloud. Besides Matlab, some auxiliary program is needed for the surface impedance definitions. Before the actual computation, a mesh definition file and a surface impedance category file, in addition to the surface impedance files, have to be created before using the actual Matlab-interface.

References

1. Waveller Cloud User Manual 14.6.2013. Kuava Ltd. 7 p.
2. Järvenpää, S. & Ylä-Oijala, P., CompA Algorithm – Mathematical Background. Edt. Huttunen, T., Kuava Oy. January 31, 2011. 16 p.
3. CompA ASCII Format. Definitions of the file format for the ASCII interface. Kuava Oy. 12 p.
4. Personal communication, Tomi Huttunen, Kuava Oy.
5. Uosukainen, S., Acoustic field theory. Espoo: Aalto University, Science + Technology 17/2013, 2013. 633 p. In Finnish
6. Skudrzyk, E., The Foundations of Acoustics. Springer–Verlag, Wien 1971. 790 p.
7. Lindell, I., Sähkömagnetiikan matemaattiset menetelmät. Espoo: Technical University of Helsinki, 1976. 151 p.
8. Filippi, P. J. T., Layer potentials and acoustic diffraction. J. Sound Vib. 54(1977)4, 473–500.
9. Fahy, F. & Gardonio, P., Sound and Structural Vibration. Elsevier, Amsterdam 2007. 633 p.
10. Van Bladel, J., Electromagnetic Fields. Hemisphere Publishing Corporation 1985. 556 p.
11. Harrington, R. F., Field Computation by Moment Methods. The Macmillan Company, 1968. 229 p.
12. Bathe, K.-L., Finite Element Procedures in Engineering Analysis. Prentice–Hall, Inc., New Jersey 1982. 735 p.
13. Oden, J. T. & Reddy, J. N., Variational Methods in Theoretical Mechanics. Springer–Verlag, Berlin 1976. 302 p.
14. Burton, A. J. & Miller, G. F., The application of integral equation methods to numerical solutions of some exterior boundary value problems. Proc. Royal Soc. London Ser A, 323(1971), pp. 201–210.
15. Schenck, H. A., Improved integral formulation for acoustic radiation problems. J. Acoust.Soc. Am. 44(1968), pp. 41–58.
16. Malinen, M., Partitioned analysis procedures for viscous cavities II: Progress report, CSC – Scientific Computing Ltd.
17. Saad, Y. & Schultz, M. H., GMRES: a generalized minimal residual algorithm for solving nonsymmetric linear systems. SIAM Journal of Scientific and Statistical Computing 7(1986), pp. 856–869.
18. http://en.wikipedia.org/wiki/Generalized_minimal_residual_method.
19. http://en.wikipedia.org/wiki/Krylov_subspace.
20. http://en.wikipedia.org/wiki/Arnoldi_iteration.
21. Saad, Y., Iterative Methods for Sparse Linear Systems. PWS Publishing, New York 1996.
22. Sloan, S. W., An algorithm for profile and wavefront reduction of sparse matrices. Int. J. for Numerical Methods in Engineering 23(1986), pp. 239–251.
23. Sloan, S. W., A Fortan program for profile and wavefront reduction. Int. J. for Numerical Methods in Engineering 28(1989), pp. 2651–2679.
24. Coifman, R., Rokhlin, V. & Wanzura, S., The fast multipole method for the wave equation: a pedestrian prescription. IEEE Antennas Propagation Magazine 35(1993)3, pp. 7–12.
25. Chew, W. C., Jin, J.-M., Michielssen, E. & Song, J., Fast and Efficient Algorithms in Computational Electromagnetics. Artech House, Boston 2001.
26. Song, J. M. & Chew, W. C., Multilevel fast-multipole algorithm for solving combined field integral equations of electromagnetic scattering. Microwave Opt. Tech. Lett. 10(1995), pp. 14–19.
27. Michielssen, E. & Chew, W. C., Fast steepest descent path algorithm for analyzing scattering from two-dimensional objects. Radio Science 31(1996)5, pp. 1215–1224.

28. Greengard, L., Huang, J., Rokhlin, V. & Wadsura, S., Accelerating fast multipole methods for the Helmholtz equation at low frequencies. IEEE Computations in Sciences and Engineering 5(1998)3, pp. 32–38.
29. Jiang, L. J. & Chew, W. C., Low-frequency fast inhomogeneous planewave algorithm (LFFIPWA). Microwave Opt. Tech. Lett. 40(2004)2, pp. 603–628.
30. Wallén, H., Järvenpää, S. & Ylä-Oijala, P., Broadband multilevel fast multipole algorithm for acoustic scattering problems. J. Comp. Ac. 14(2006)4, pp. 507–526.
31. Wallén, H, & Sarvas, J., Translation procedures for broadband MLFMA. Progress in Electromagnetics Research, PIER 55(2005), pp.47–78.
32. Wallén, H., Improved interpolation of Evanescent plane waves for fast multipole methods. PIERS Online 3(2007)6, pp. 764–766.
33. Siponen, D., Lehtinen, A. & Uosukainen, S., NOVI – Advanced functional solutions for Noise and Vibration reduction of machinery, deliverable D2.3: Virtual cabin model. Espoo: VTT. 2013.
34. Actran 12.1 User's Guide. Volume 1: Installation, operations, theory and utilities. Free Field Technologies SA, 2012. 587 p.